Environment International 171 (2023) 107649

Contents lists available at ScienceDirect

Environment International

journal homepage: www.elsevier.com/locate/envint

Full length article

Association between temperature variability and global meningitis incidence

Junjun Chen [a], Zhihua Jiao [b], Zhisheng Liang [c], Junxiong Ma [c], Ming Xu [c,d], Shyam Biswal [e], Murugappan Ramanathan [f], Shengzhi Sun [g], Zhenyu Zhang [c,d,*]

[a] Department of Electrical and Computer Engineering, Johns Hopkins University, Baltimore, MD, USA
[b] Department of Cell Biology, Johns Hopkins University School of Medicine, Baltimore, MD, USA
[c] Department of Global Health, Peking University School of Public Health, Beijing, China
[d] Institute for Global Health and Development, Peking University, Beijing, China
[e] Environmental Health and Engineering, Johns Hopkins Bloomberg School of Public Health, Baltimore, US
[f] Department of Otolaryngology-Head and Neck Surgery, Johns Hopkins University School of Medicine, Baltimore, MD, USA
[g] School of Public Health, Capital Medical University, Beijing, China

ARTICLE INFO

Handling Editor: Adrian Covaci

Keywords:
Temperature variability
Meningitis
GBD
Shared Socioeconomic Pathways
Climate Change

ABSTRACT

Background: Meningitis can cause devastating epidemics and is susceptible to climate change. It is unclear how temperature variability, an indicator of climate change, is associated with meningitis incidence.
Methods: We used global meningitis incidence data along with meteorological and demographic data over 1990–2019 to identify the association between temperature variability and meningitis. We also employed future (2020–2100) climate data to predict meningitis incidence under different emission levels (SSPs: Shared Socioeconomic Pathways).
Results: We found that the mean temperature variability increased by almost 3 folds in the past 30 years. The largest changes occurred in Australasia, Tropical Latin America, and Central Sub-Saharan Africa. With a logarithmic unit increase in temperature variability, the overall global meningitis risk increases by 4.8 %. Australasia, Central Sub-Saharan Africa, and High-income North America are the most at-risk regions. Higher statistical differences were identified in males, children, and the elderly population. Compared to high-emission (SSP585) scenario, we predicted a median reduction of 85.8 % in meningitis incidence globally under the low-emission (SSP126) climate change scenario by 2100.
Conclusion: Our study provides evidence for temperature variability being in association with meningitis incidence, which suggests that global actions are urgently needed to address climate change and to prevent meningitis occurrence.

1. Introduction

Meningitis is an inflammation of the membranes (meninges) covering the brain and the spinal cord, usually caused by bacterial, viral, fungal, or parasitic infection (Collaborators, 2018; Wright et al., 2021). The severity of meningitis alters with the causative organism (Erdem et al., 2017). For example, viral meningitis, the most common type of this disorder, can occur throughout the year, mostly in summer and autumn. It usually affects young children, potentially leading to severe complications such as high fever, mental retardation, and even death in extreme cases (Kohil et al., 2021). As of 2019, the number of global meningitis new cases of all causes was estimated to be 2.51 million, and the worldwide incidence rate was 32.4 new cases per 100 k population (GBD, 2019). Apart from the tremendous health burden of meningitis on mortality and morbidity, this disease also has a severe socioeconomic impact on patients' income and education (Pickering et al., 2018).

Numerous factors can affect the occurrence of meningitis. Among these, climatic variability and seasonality play an essential role in the spatiotemporal distribution of the disease. Vectors rely heavily on suitable habitats and climatic conditions to propagate (Henne et al., 2018). Because of which, meningitis transmission is highly seasonal: occurrences have been more prevalent in recent years due to climate change (Ayanlade et al., 2020). Studies have identified that climate change is likely to increase the incidence of meningitis, as raised temperature

* Corresponding author at: Department of Global Health, The Peking University School of Public Health, 38 Xueyuan Rd, Haidian Dist, Beijing, China.
E-mail address: zzy@pku.edu.cn (Z. Zhang).

https://doi.org/10.1016/j.envint.2022.107649
Received 10 August 2022; Received in revised form 23 October 2022; Accepted 19 November 2022
Available online 21 November 2022

might enhance meningococcal defense against human immune killing (Loh et al., 2013). A survey on meningitis in Ghana revealed that hot season, extreme rainfall, drought, flooding, and dusty conditions could affect meningitis outbreaks. In particular, the disease occurs during drought, which usually comes with extreme heat and dusty conditions (Codjoe and Nabie, 2014). Several similar studies on the meningitis belt (a region of Sub-Saharan Africa) also concluded that humidity, dust, and rainfall are associated with meningitis epidemics (Cuevas et al., 2007; Molesworth et al., 2003). Another study reported that seasonal winds were the main climatic driver behind the meningitis belt, and a high disease incidence was correlated to dry, windy, and dusty conditions (Sultan et al., 2005). Global warming will change climate patterns with more intense droughts in some locations and more frequent heavy rainfall in other places (Pörtner et al., 2022).

Previous studies on the association between climate and meningitis occurrence focus primarily on the classical endemic areas, i.e., the meningitis belt and other highincidence regions (Ayanlade et al., 2020; Codjoe and Nabie, 2014; Sultan et al., 2005; Palmgren, 2009; Analysis of the Effect of Temperature on Age and Sex Incidence of Cerebro-Spinal Meningitis in Funtua Local Government Area and State, 2021; Abdussalam et al., 2014; Abdussalam et al., 2014; Yaka et al., 2008). While the climate and seasonal changes are of great interest to researchers, very little attention has been directed at temperature and climate variability, which can be strong indicators of climatic variations and forewarns of upcoming extreme weather events (Lenton et al., 2008; Bathiany et al., 2018). To our knowledge, prior studies using temperature and climatic variability as indices for identifying the association with meningitis are limited to a single local study area and to a relatively short period of up to 10 years, no study has estimated the association between temperature variability and meningitis on a global scale and over a long period (Buhari, 2011; Adebayo, 2001). Furthermore, few studies have explored future meningitis incidence trends at different greenhouse gas emission levels and under different climate policies, which can be represented by Shared Socioeconomic Pathways (SSPs). These pathways are projected scenarios of global socioeconomic changes to 2100. With the severity ranked from low to high, SSP126 stands for a scenario where humanity chooses a sustainable low carbon way of life, leading to reduced global warming by 2100; On the contrary, SSP585 depicts a tougher scenario where greenhouse gas emissions continue to rise, causing a higher level of global warming; SSP245 and SSP370 are considered as the medium stabilization scenarios, representing the middle of the green road.

Here, we proposed to use temperature variability derived from the optimum maximum temperatures of 204 countries/locations over 1990–2019 to identify the association between temperature variability and meningitis occurrence and to quantify the risks faced by each region. Using multi-model ensemble (MME) meteorological data, a method that integrates various climate models' prediction results, we would also project the changes in future temperature variability and meningitis incidence rate (2020–2100) under different Shared Socioeconomic Pathways (SSP: 126, 245, 370, and 585). We hypothesized that places with elevated temperature variability and high greenhouse gas emission level would be at increased risk of meningitis incidence compared to those with lower temperature variability and controlled emissions.

2. Methods

2.1. Data sources

The Global Burden of Disease (GBD) is one of the most comprehensive studies to date that provides a powerful resource for researchers to quantify global health loss due to hundreds of diseases, injuries, and risk factors (GBD, 2019). It has epidemiological data from more than 350 diseases and injuries in 195 countries by sex and age between 1990 and 2019 (Diseases and Injuries, 2020; Collaborators, 2020). Meningitis was categorized into four sub-causes, including *N meningitides* (meningococcal), *S pneumonia* (pneumococcal), *H influenzae* type b, and other pathogens (bacteria, fungi, viruses, etc.). Incidence attributable to meningitis was linked to the GBD cause list with the following International Classification of Diseases and Injuries, ninth and tenth Revision (ICD-9 and ICD-10) codes: 036–036·9/A39–A39·9 (meningococcal meningitis), 320·1/G00·1 (pneumococcal meningitis), 320·0/G00·0 (H influenzae type b meningitis), and 047–049/320·2–322·9 (other meningitis) (Collaborators, 2018). All incidences of four sub-causes were grouped into a single value to represent the total meningitis incidence by the GBD researchers. Further data collection, processing, analysis, and modelling details are available in the GBD 2019 publication (Collaborators, 2020).

TerraClimate is a global gridded database of climate variables at a monthly temporal resolution of $\sim$ 4 km from 1958 to the present (Abatzoglou et al., 2018; Zhao et al, 2022; Lobell et al., 2022). In addition to providing first-order climate variables such as maximum temperature, minimum temperature, precipitation accumulation, and wind speed, TerraClimate also offers derived climate variables, including soil moisture, snow water equivalent, runoff, etc.

Our study used the sociodemographic index (SDI), which represents the country's average years of schooling, income per capita, and fertility rate in females under 25 years old (Diseases and Injuries, 2020). Based on the geographical distribution, cultural characteristics, and local conventions, 204 GBD countries/locations were categorized into 21 GBD geographical regions (**Supplementary Table 2**).

Utilizing shapefiles of GBD country's first-level administrative areas, we extracted the primary climate data (maximum temperature) and other meteorological risk factors (soil moisture, precipitation, and wind speed) from the TerraClimate raster data. Because the GBD only provided the annual estimates, we calculated each country's annual estimates of the climatic predictors. The top 4 highest monthly temperatures of each year were averaged as the maximum temperature for that year, accounting for seasonal and geographical differences (Sultan et al., 2005; Ma et al., 2021). Twelve months of soil moisture, precipitation, and wind speed measurements were averaged to represent their annual values. Meningitis incidence rate data of 204 countries/locations, stratified by sex and age, were sourced from the GBD database. The SDI is a time-varying indicator, i.e., one country may have had a middle SDI in 1990 but a high SDI in 2019. The latest 2019 SDI values, for their better representativeness, were adopted in this study.

We used a similar approach as mentioned above (masking using shapefiles of GBD countries) to extract maximum temperature and precipitation from The Coupled Model Intercomparison Project Phase 6 (CMIP6) data, which provide past, present, and future climate data in a multimodal framework (Eyring et al., 2016; Petrie et al., 2021). Five widely-employed representative climate models (ACCESS-CM2, CanESM5, IPSL-CM6A-LR, MIROC6, UKESM1-0-LL) were selected, downscaled, and bias-corrected with WorldClim v2.1, a widely used historical climate dataset over 1970–2000, as the baseline climate (Fick and Hijmans, 2017). Monthly values of maximum, minimum temperature, and precipitation were generated for four SSPs (126, 245, 370, and 585). These values were averaged over 20-year periods (2021–2040, 2041–2060, 2061–2080, and 2081–2100).

2.2. Statistical method

We adopted a three-step analysis strategy. First, generalized linear regression models adjusted for year, age, and sex were built to estimate the dose–response relationship between maximum temperature and incidence rate of meningitis for each GBD country. The maximum temperature with the lowest incidence rate of meningitis would be identified as the "ideal" baseline temperature, at which the disease is most unlikely to occur in the population. Using this location-specific baseline temperature value, the absolute maximum temperature differences from the "ideal" temperature of each country from 1990 to 2019 were calculated as the maximum temperature variability value.

For the second step, we used a generalized linear regression model to preliminarily screen the associations between meningitis incidence and all climate variables respectively. Those with statistical differences were included in the following analysis. Next, we began our generalized additive regression modeling with only meningitis incidence and temperature variability, which were found to be the most significant climate risk factor of all the variables. By using the likelihood-ratio test, we took a forward stepwise feature selection technique to compare models, as well as to check and incorporate any variable that had statistical difference. We selected important climate variables and chose the proper degree of freedom for each spline term. In the fully adjusted model, we adjusted for relevant demographic, socioeconomic, and meteorological covariances such as sex, age, SDI, soil moisture, precipitation, and wind speed. A natural cubic spline was applied to soil moisture and precipitation with a freedom of 3. These regions would allow a more straightforward generalization of places most susceptible to increased extreme temperature variability. Subgroup and sensitivity analyses by age, sex, and SDI stratification were conducted according to the potential risk factors.

In the third prediction step, we resorted to a common yet effective approach called the multi-model ensemble (MME) to minimize future climate models' uncertainties and to improve prediction accuracy. It is a technique that integrates multiple models' prediction results as an ensemble. Studies on precipitation projections over China have reported that the bias of the MME was much lower than that of individual CMIP6 models (Tian et al., 2021). We believe that this finding, an ensemble performs better than a single model alone, also applied to MME in other regions of the world. To fully exploit the advantages of each model as well as to minimize model structural errors and parameterization uncertainties as much as possible, our improved MME approach was to calculate the 10th, 50th (ensemble median), and 90th percentile for all models' prediction values as the range of changes. Then, repeat for all SSP scenarios over 2020–2100. To ensure a smooth transition from past data to future projection, we also computed meteorological data from 2000 to 2020. We assumed that the optimum temperature at which the incidence rate was the lowest would remain the same in the future, and the demographic composition of the study population would change barely. Relying on this assumption, location-specific data from 2000 to 2020 were used as the baseline to calculate the maximum temperature variability over 2020–2100. These data and other CMIP6 future meteorological data were fed into the model we developed in step two to generate projections and their ranges of predicted changes under four SSP scenarios.

3. Results

Between 1990 and 2019, the global mean incidence rate per 100 k population was 46.2, ranging from 5.9 in High-income North America to 218.5 in Western Sub-Saharan Africa (Table 1). The global mean maximum temperature is 29.4 ℃, with the lowest at 11.8 ℃ in High-income North America and the highest at 37.0 ℃ in North Africa and Middle East. The global average soil moisture, precipitation, and wind speed are 66.7 mm (range between 9.3 and 147 mm), 103.8 mm (17 to 228.8 mm), and 2.9 m/s (1.8 to 4.1 m/s), respectively.

From 1990 to 2019, the temperature variability reached a small peak of approximately 0.68 ℃ in the mid-1990 s. It started to decrease to 0.62 ℃ in the mid-2000 s and continued to fluctuate until 2010 when it then increased gradually again (Fig. 1**A**). We found that the changes in temperature variability varied considerably across different countries and regions. Over the last 30 years, the global value has increased by approximately three times. Australasia has the highest increase in temperature variability by 22.16-fold, followed by Tropical Latin America, which increased by 12.91-fold, and Central Sub-Saharan Africa, which increased by 10.99-fold (Fig. 1**B**). Based on the average temperature variability over 1990 to 2019, we observed that certain countries and regions have a relatively higher temperature variability between 0.86 ℃ and 1.70 ℃ (Fig. 1**C**). There is a clear pattern of the meningitis belt that spans from Western Sub-Saharan Africa to Eastern Sub-Saharan Africa. The incidence rates experienced in the "belt" are significantly higher than those in other parts of the world. The incidence rates in Europe and the Americas both remain relatively low, while sporadically, the incidence can be slightly high in Central Asia and South/Southeast Asia. The incidence rates do not always correspond to the countries' mean temperature variability (Fig. 1**C**).

In the preliminary association screening between meningitis incidence and climate variables, temperature variability, precipitation, and wind speed showed high statistical differences, except for soil moisture (**Supplementary Table 1**). Among all significant factors, temperature variability demonstrated the most notable effect (1.04, 95 % CI: 1.03–1.04, $p < 0.001$) on meningitis incidence, compared to that of

Table 1
The characteristics of meningitis incidence and climatic factors from 1990 to 2019 by GBD region.

Regions	Incidence rate	Max temperature (°C)	Soil moisture (mm)	Precipitation (mm)	Wind speed (m/s)
Global	46.2 (9.8)	29.4 (6.4)	66.7 (62.2)	103.8 (75.6)	2.9 (1.1)
East Asia	9.1 (5.3)	25.6 (1.7)	47.4 (14.4)	124.4 (73.5)	3.5 (1.1)
Central Asia	42 (10.6)	25.9 (5.5)	22.1 (17.3)	35.6 (23.8)	2.7 (1)
South Asia	69.2 (20.1)	29.0 (6.2)	85.1 (48.7)	102.4 (53)	4.0 (1.4)
Southeast Asia	29.9 (9.3)	31.1 (1.4)	134.6 (77.5)	168.9 (46.1)	2.8 (1.3)
Highincome Asia Pacific	19 (3.5)	28.0 (3.8)	53.4 (18.3)	181.8 (88.9)	3.6 (1.3)
Oceania	67.7 (12.1)	30.4 (1)	46.8 (21.6)	228.8 (79.1)	2.9 (0.7)
Australasia	14.6 (3.1)	27.1 (7.4)	44.8 (21.7)	88.3 (51)	1.8 (0.2)
Andean Latin America	11.3 (4.1)	27.1 (1.5)	86.3 (15.6)	135.4 (41.9)	3.6 (1.1)
Tropical Latin America	34.8 (7.8)	32.3 (1.2)	86.3 (62.5)	118.0 (28.1)	4.1 (0.5)
Central Latin America	12.5 (5.5)	31.1 (1.1)	147.3 (48.6)	171.9 (53.3)	3.0 (1)
Southern Latin America	14.6 (4.5)	24.7 (5)	36.4 (17.6)	82.1 (29.3)	3.2 (1.6)
Caribbean	28.9 (6.3)	31.1 (0.9)	85.0 (80.6)	140.5 (37.1)	2.9 (0.8)
Highincome North America	5.9 (2.1)	11.8 (11.8)	33.2 (12.7)	48.4 (8.3)	3.9 (1)
Central Europe	11.9 (3.2)	24.5 (1.8)	62.0 (20.6)	70.8 (25.1)	3.3 (1.1)
Western Europe	12.2 (3)	22.4 (6.3)	53.9 (23.9)	72.1 (23.6)	3.0 (1.2)
Eastern Europe	20.6 (3.7)	21.5 (2.9)	60.3 (22)	50.2 (9.2)	2.1 (0.7)
North Africa and Middle East	30.4 (7)	37.0 (4.3)	9.3 (16.5)	17.0 (16.6)	2.8 (1)
Western Sub-Saharan Africa	218.5 (56.4)	35.6 (3.7)	105.2 (93.8)	100.0 (70.3)	2.8 (1)
Eastern Sub-Saharan Africa	165.7 (41.4)	31.9 (3.4)	57.4 (40.6)	77.6 (38.4)	2.3 (0.6)
Southern Sub-Saharan Africa	55.7 (6.5)	30.0 (3.3)	11.9 (12)	45.1 (17.8)	2.9 (1.1)
Central Sub-Saharan Africa	151.7 (33.8)	31.1 (1.7)	119.5 (40.6)	135.4 (33.1)	3.1 (1.2)

Region-specific incidence rate values were sourced from the GBD database, and the other values were calculated as the average (SD) of 1990 to 2019 using TerraClimate meteorological annual data. The incidence rate is the number of new cases per 100 k population. The maximum temperature was the average of the hottest 4 months of the year; soil moisture, precipitation, and wind speed were the annual means.

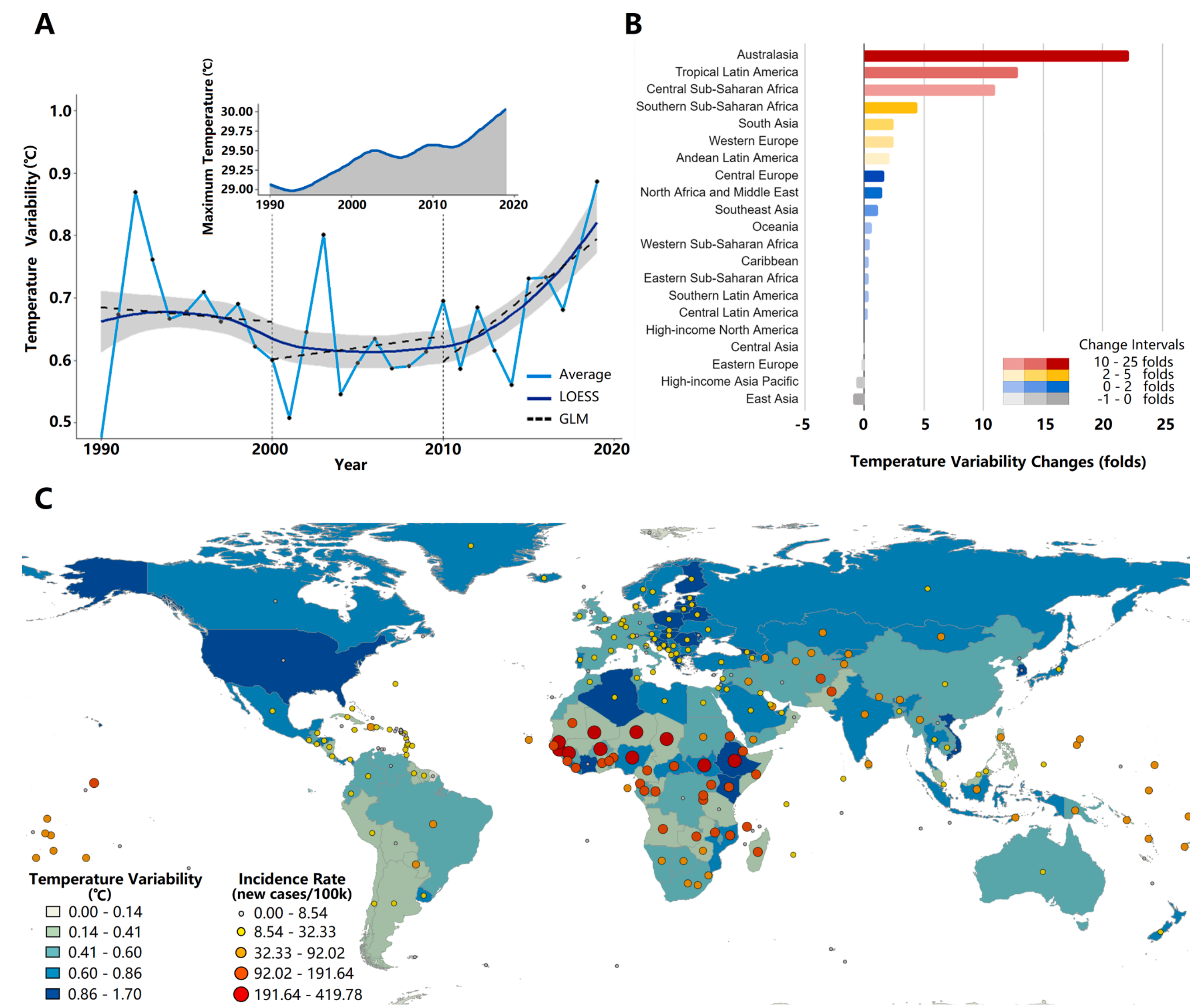

Fig. 1. Changes in global, regional, and local mean temperature variability and the incidence rate of meningitis from 1990 to 2019. **(A)** Temporal changes in average temperature variability (light blue line on the main plot), long-term trends for each interval (1990 s, 2000 s, 2010 s) of the mean temperature variability (black dashed line) using GLM (generalized linear model), and smoothed average temperature variability with its 95 % confidence interval (dark blue line and the gray shading on the main plot) using LOESS (Locally Weighted Linear Regression); time-series of mean annual maximum temperature over 1990–2019 (blue line with gray shading on the side plot). **(B)** Regional temperature variability changes compared to 1990 in descending order, with each color scale representing the magnitude of changes: red for increases greater than 10, yellow for increases greater than 2 and<5, blue for increases between 0 and 2, and gray for decreases between −1 and 0. **(C)** Global map of local mean temperature variability over 1990–2019 with 5 intervals ranging from 0.14 to 1.70 ℃ and color-scaled dots showing the severity of the local mean incidence rate (ranging from 5.93 to 419.78 new cases per 100 k population) of each country over 1990–2019. (For interpretation of the references to color in this figure legend, the reader is referred to the web version of this article.)

precipitation (0.99, 95 % CI: 0.99–0.99, $p < 0.001$) and wind speed (1.02, 95 % CI: 1.02–1.02, $p < 0.001$). Wind speed, as we assumed that can heavily affect meningitis incidence, was found to have a strong association, but the effect was only about half compared to that of temperature variability. Precipitation, on the other hand, was identified to be a protective factor. We also noticed that despite soil moisture showing the negligible statistical difference, including it in the final model still improved the model's explanatory power. We could now preliminarily confirm and consider temperature variability as the main risk factor compared to other climate variables.

In the fully adjusted model, we found that for each logarithmic unit increase in temperature variability, the risk of meningitis increased by 5.0 % (OR, 1.05; 95 % CI: 1.05–1.05) globally (Table 2). For each logarithmic unit increase in temperature variability, the risks of meningitis for Australasia, High-income North America, and Central Sub-Saharan Africa were 20 % (OR, 1.20; 95 % CI: 1.19–1.22), 16 % (OR, 1.16; 95 % CI: 1.14–1.18), and 14 % (OR, 1.14; 95 % CI: 1.12–1.16), respectively. We did not find an association in Southern Latin America, North Africa and Middle East, Eastern Sub-Saharan Africa, or Southern Sub-Saharan Africa. Increased temperature variability is a protective factor for Central Asia (OR, 0.96; 95 % CI: 0.95–0.98) and Oceania (OR, 0.98; 95 % CI: 0.97–0.99). We also observed significant associations ranging from 3 % in South Asia (OR, 1.03; 95 % CI: 1.01–1.05) and Eastern Europe (OR, 1.03; 95 % CI: 1.01–1.05) to 8 % in Tropical Latin America (OR, 1.08; 95 % CI: 1.06–1.10) and Western Europe (OR, 1.08; 95 % CI: 1.06–1.09).

We found that sex and age may be modifiers of the effect of temperature variability on the risk of meningitis. For each logarithmic unit increase in temperature variability, males had an increased risk of 5 %

Table 2
Association of climate factors with meningitis incidence rate from 1990 to 2019 by GBD region.

Regions	OR (95 % CI)	P value
Global	1.05 (1.05, 1.05)	<0.001
East Asia	Ref	Ref
Central Asia	0.96 (0.95, 0.98)	<0.001
South Asia	1.03 (1.01, 1.05)	<0.001
Southeast Asia	1.05 (1.03, 1.06)	<0.001
High-income Asia Pacific	1.06 (1.04, 1.08)	<0.001
Oceania	0.98 (0.97, 0.99)	0.01
Australasia	1.20 (1.18, 1.22)	<0.001
Andean Latin America	1.07 (1.05, 1.09)	<0.001
Tropical Latin America	1.08 (1.06, 1.10)	<0.001
Central Latin America	1.04 (1.02, 1.05)	<0.001
Southern Latin America	1.01 (0.99, 1.03)	0.38
Caribbean	1.06 (1.05, 1.08)	<0.001
High-income North America	1.16 (1.14, 1.18)	<0.001
Central Europe	1.05 (1.03, 1.06)	<0.001
Western Europe	1.08 (1.06, 1.09)	<0.001
Eastern Europe	1.03 (1.01, 1.05)	<0.001
North Africa and Middle East	1.00 (0.99, 1.02)	0.63
Western Sub-Saharan Africa	1.03 (1.02, 1.05)	<0.001
Eastern Sub-Saharan Africa	1.01 (0.99, 1.02)	0.34
Southern Sub-Saharan Africa	1.00 (0.99, 1.02)	0.66
Central Sub-Saharan Africa	1.14 (1.12, 1.16)	<0.001

East Asia was chosen as the reference because it has the largest population and mild changes in temperature variability compared to all other regions. Maximum temperature, year, sex, age, region, soil moisture, precipitation, and wind speed were adjusted for the final model.

(OR, 1.05; 95 % CI: 1.04–1.05), while females had a decreased risk of 1 % (OR, 0.99; 95 % CI: 0.98–0.99). For stratified age groups, we noticed that children and elderly adults had higher risks than mid-aged adults, with an OR of 1.10 (95 % CI: 1.09–1.12) for the 1- to 4-year-old age group and 1.02 (95 % CI: 1.01–1.03) for the 75- to 79-year-old age group. This study did not find any difference between the SDI groups (Fig. 2).

Under all greenhouse gas emission scenarios, future changes in temperature variability would increase linearly to approximately 2040 and diverge according to different scenarios. We found that the lowest emission pathway, SSP126, has the most modest increase in temperature variability. Along this pathway, temperature variability increases to 2040 and peaks around the mid-2070 s, reaching a median total increase of below 2.5-fold (CI: 1.4–2.9 folds). From the 2070 s onwards, the temperature variability level of SSP126 remains at a low and stable level of about 2.2 folds (CI: 1.2–2.7 folds). In comparison, SSP370 and SSP585 increase at a much faster rate. The former reaches the highest point of 7.5-fold (CI: 4.5–9.0 folds) by 2100, whereas SSP585, the highest emission counterpart, has the most significant increase in temperature variability, with a substantial increase of close to 10-fold (CI: 7.0–11.5 folds) by the end of the century (Fig. 3**A**). The changes in future incidence rates shared a similar pattern of temperature variability for the four future emission scenarios. Under SSP126, because of the stricter control of future greenhouse gas emissions, the meningitis incidence rate will increase by 25 % (CI: 15 %-35 %) until the 2040 s at a gradually slower pace of change and will begin declining past the 2070 s. However, in contrast to mild changes in the SSP126 scenario, the higher greenhouse gas emission level of the SSP585 scenario would experience a worsened situation starting from the 2060 s, as the increase in

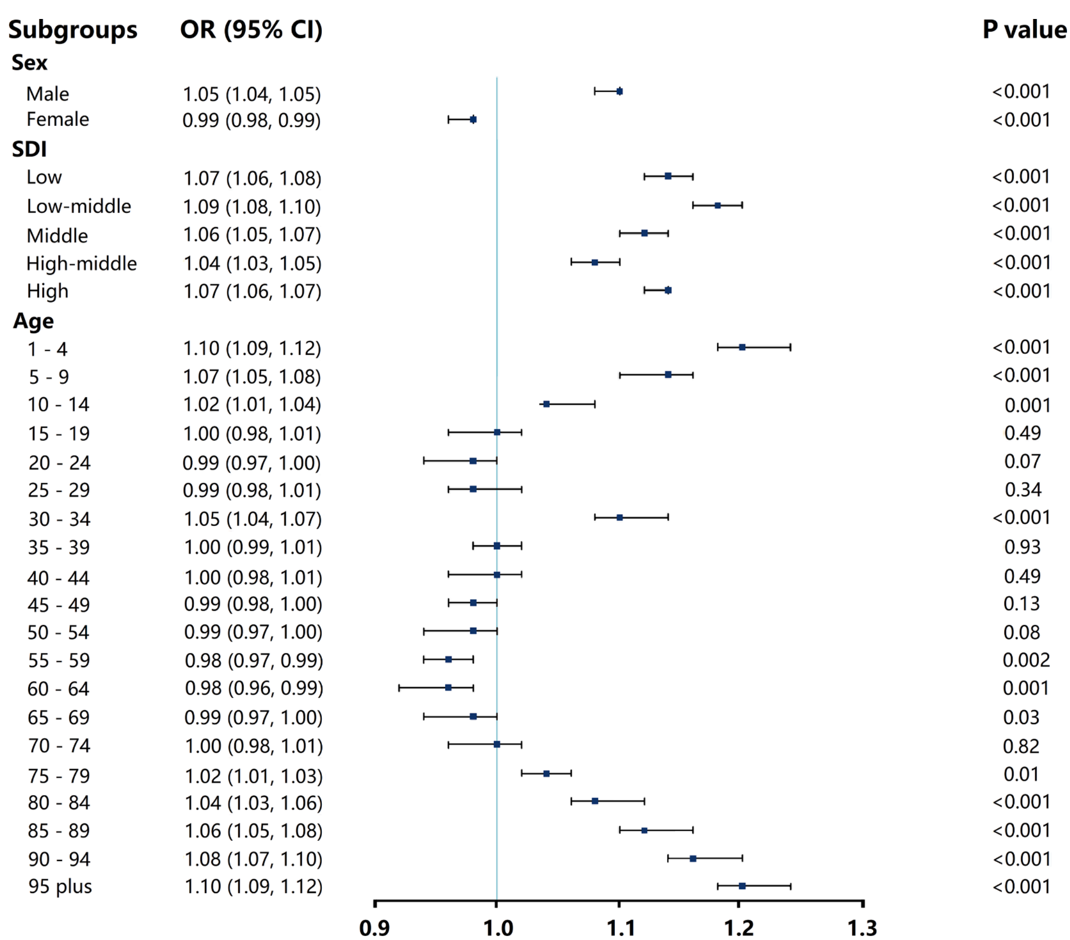

Fig. 2. Subgroup analysis of covariates vs temperature variability. Models were adjusted for year, sex, age, region, soil moisture, precipitation, wind speed, and the interaction term between temperature variability and the respective reference subgroups.

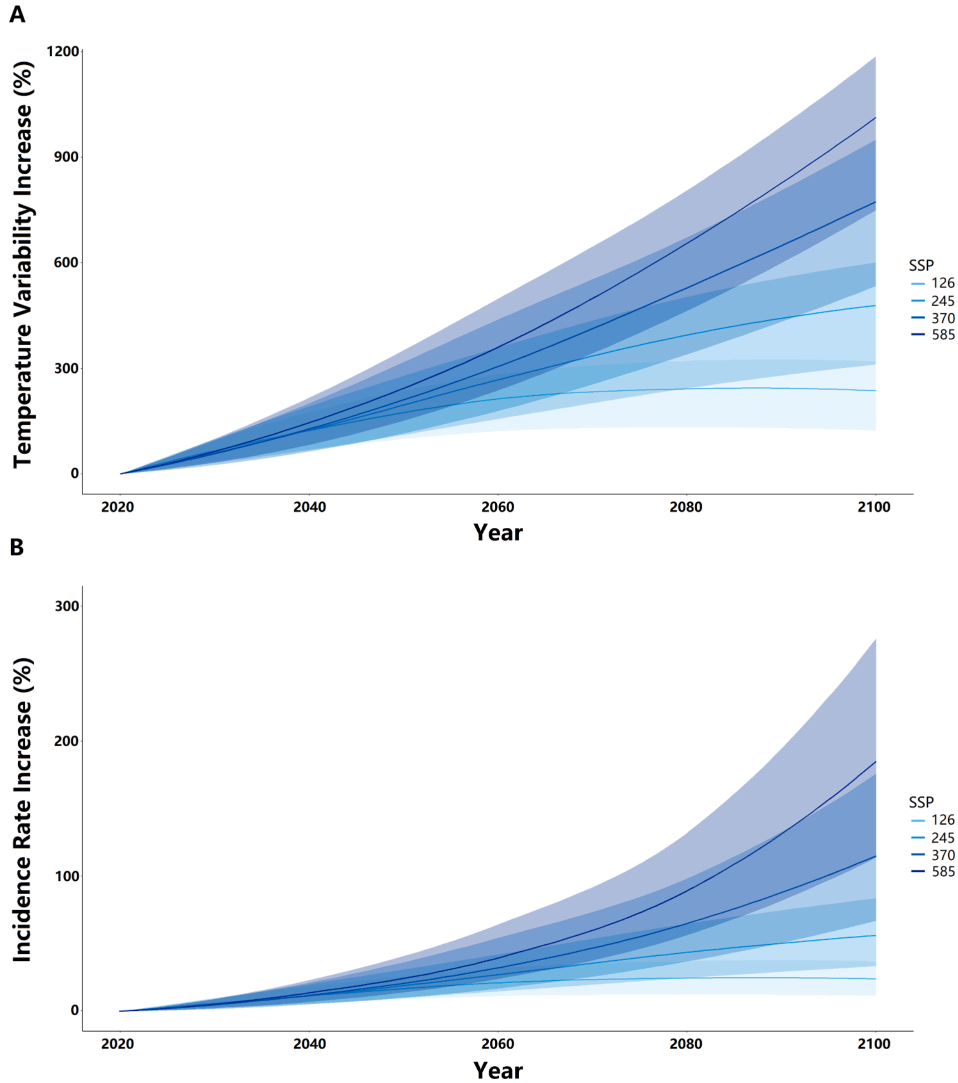

Fig. 3. Multi-model ensemble (MME) projections of future increases in **(A)** temperature variability and **(B)** meningitis incidence compared to the base year 2020 under different Shared Socioeconomic Pathway (SSP) scenarios: SSP126, SSP245, SSP370, and SSP585. Solid curves represent the MME median, and the ranges of each model fall within the 10th and 90th percentile.

meningitis incidence of SSP585 would experience a substantially faster rate of change, resulting in a final rise of well over 180 % (CI: 100 %-290 %) by 2100 (Fig. 3**B**). The median incidence rate of SSP126 is predicted to be only 25.8 by 2100 and that of SSP585 will be 182.0 by 2100. The SSP126 scenario would see a median of 85.8 % reduction compared to the SSP585 scenario by 2100.

4. Discussion

We found that the incidence of meningitis is associated with temperature variability, and the associations were more announced in males, children, and the elderly population. Temperature variability derived from maximum temperature is crucial to evaluate the severity and frequency of climate change, especially extreme weather events such as extended droughts and heavy precipitation. The epidemiology of meningitis is closely related to climatic factors such as air humidity, rainfall, wind, and dust. Our findings agreed with previous studies on the meningitis belt that countries within the region, particularly much of Central and Western Sub-Saharan Africa, continue to have a high burden of meningitis (Collaborators, 2018; Codjoe and Nabie, 2014; Cuevas et al., 2007). We also validated that these regions are at the highest risk for meningitis affected by increasing temperature variability. Several other new areas vulnerable to changes in temperature variability have been identified: Australasia and High-income North America. The United States and Australia have suffered from wildfires in recent years. According to a study on wildfires, human health, and climate change, these three factors are closely connected. Climate change can lead to rainfall anomalies, strong winds, increased lightning strikes, and high temperatures, thus leading to wildfires and longer wildfire seasons and producing more ambient air pollution (Xu et al., 2020). These climate change-induced meteorological conditions are ideal for meningitis outbreak, which requires hot, dry, and windy weather (Palmgren, 2009). Fine particulate matter and other toxic air pollutants, such as carbon monoxide, ozone, nitrogen dioxide, and hydrogen cyanide, from wildfire smoke can significantly threaten human health. In addition, the high temperature that usually comes with wildfires and oxidant gases can increase the health risks of wildfire particulate matter (Shaposhnikov et al., 2014; Lavigne et al., 2018). Exposure to such air pollutants can lead to increased asthma, chronic obstructive pulmonary disease, and respiratory infection (Reid et al., 2016; Black et al., 2017). Other studies have also suggested that dry, windy, and dusty air conditions can injure the immune barriers of the upper respiratory tract mucosa and nasal cavity, thus facilitating meningitis infection (van Deuren et al., 2000; Moore, 1992). For example, *N. meningitidis* can more easily penetrate damaged mucosal membranes through the bloodstream and the meninges. To some extent, we know that this finding of increased meningitis risk is counterintuitive because Australia had the lowest incidence of 0.5 cases per 100,000 population (Collaborators, 2018) and a similar number of 0.2–4 per 100,000 in the USA (Harrison et al., 2009). However, this discrepancy underscores the importance of proper public health measures in containing the disease outbreak.

While meningitis typically ceases its occurrence as the wet season begins or as rainfall increases (Greenwood et al., 1984), certain at-risk regions do not fit this pattern. For example, Tropical Latin America and Southeast and South Asia feature a hot but humid climate. However, if temperature variability increases, these regions have a relatively high increase in meningitis risk. One similarity these places share is that they all have low to middle SDIs, which may reflect the lower effectiveness of their healthcare system and the lower extent of vaccination. Moreover, Australasia and High-income North America, which have high SDIs in comparison, although being found to have a high susceptibility to meningitis risk, only experience a low incidence rate, which to a certain degree reasserts the crucial role of proper public health prevention and intervention.

Depending on the future greenhouse gas emissions level, the Shared Socioeconomic Pathways are divided into four scenarios from low to high: SSP126, SSP245, SSP370, and SSP585. The lowest emission scenario, SSP126, where strict and proper actions are taken to address climate change, is the most favorable regarding acceptable mild increases in temperature variability and meningitis incidence. Based on the projections, both metrics would cease to increase in the mid-century and remain at a stable and relatively low level. At the same time, the highest emission scenario, SSP585, is projected to cause a substantial increase in temperature variability and the meningitis incidence rate. This distinct contrast again emphasizes the importance and urgency of global actions to address climate change.

Compared to other studies on meningitis, this is the first to identify and quantify meningitis risk associated with climate change-induced temperature variability on a global scale. Previous studies were constrained to the classical epidemic areas near the meningitis belt and with contiguous high incidence regions (Ayanlade et al., 2020; Codjoe and Nabie, 2014; Sultan et al., 2005; Palmgren, 2009; Analysis of the Effect of Temperature on Age and Sex Incidence of Cerebro-Spinal Meningitis in Funtua Local Government Area and State, 2021; Abdussalam et al., 2014; Abdussalam et al., 2014; Yaka et al., 2008). Additionally, while most research has focused more on climate and seasonal changes, limited attention has been directed at temperature variability, which can be a solid indicator, predictor, and risk factor for climatic variations (Lenton et al., 2008; Bathiany et al., 2018). Furthermore, prior studies using temperature and climatic variability were restricted to a small sample of a single country or to a short period of 10 years (Buhari, 2011; Adebayo, 2001). From a global perspective, our study validated regions that are traditionally at risk and discovered new areas that are also at risk and were overlooked in the past. By identifying and prioritizing these vulnerable regions and guiding proper prevention and intervention through public health measures, our work can facilitate actions in the Defeating Meningitis by 2030 Global Roadmap.

There are also limitations to our research, as it is heavily based on GBD disease data and future projection data. The less granular yearly data of GBD cannot reflect changes within each year and is unable to be used for fully leveraging the high temporal resolution of TerraClimate monthly data. Typically, there is a lagged effect of environmental exposure and an incubation period on meningococcal occurrence among the population. However, due to the lack of fine temporal epidemiologic data, we could not use a model that can consider this lagged effect. Moreover, GBD data only provide a generalized leading cause of meningitis instead of exact causes, such as viral, bacterial, and parasitic causes. This limits the identification of region- and location-specific causes of meningitis and hinders further exploration of the underlying incidence mechanism.

Furthermore, the GBD dataset provides most countries' data at a high administrative level, i.e., lacking fine data on provinces, states, and counties. For instance, China, although it has more than a handful of provinces, only has one incidence value per year for the entire country. Additionally, the effects of global immunization introduced around the 2010 s can barely be observed due to the lack of granular disease data. Additionally, GBD data are estimates generated based on a standardized Bayesian regression tool, which means uncertainties may occur. Countries with limited data sources typically have a wider confidence interval, indicating greater uncertainties in the estimates. It is worth noting that some countries, especially those in Africa, have insufficient primary data for diseases. Therefore, incidence estimates of various diseases, including meningitis, contain modelling results for the cause-specific model derived from data from other countries. Our future prediction results were heavily dependent on the assumption that the optimum maximum temperature for humans and the population's demographics would remain the same in the future, which could introduce some uncertainties. During the analysis of multiple CMIP6 climate models, we noticed minor disparities between each model, but these disparities should not be entirely treated as errors because no "best" meteorological model exists. In fact, the uncertainties in each model should be considered a unique and complicated mathematical representation of the climate system. Thus, employing the multi-model ensemble technique instead of the individual model alone can reduce bias to the greatest extent.

5. Conclusion

In this global-scale ecological study, we identified a strong association between temperature variability and the meningitis incidence rate. In addition, we recognized that Australasia, Central Sub-Saharan Africa, and High-income North America are most susceptible to meningitis risks with increased temperature variability. We also revealed that different Shared Socioeconomic Pathways could lead to drastically different consequences for both temperature variability and meningitis incidence rate. These results suggest that to achieve the WHO Defeating Meningitis by 2030 Global Roadmap, more urgent actions should be taken to address climate change as well as the meningitis risk posed by climate change.

6. Ethics Approval

Not applicable.

Role of the funding source

This research received no specific funding.

CRediT authorship contribution statement

Junjun Chen: Data curation, Writing – original draft, Writing – review & editing. **Zhihua Jiao:** Visualization, Investigation. **Zhisheng Liang:** Software, Validation. **Junxiong Ma:** Visualization, Investigation. **Ming Xu:** . **Shyam Biswal:** Supervision. **Murugappan Ramanathan:** Supervision. **Shengzhi Sun:** Supervision. **Zhenyu Zhang:** Conceptualization, Methodology, Software.

Declaration of Competing Interest

The authors declare that they have no known competing financial interests or personal relationships that could have appeared to influence the work reported in this paper.

Data availability

Data will be made available on request.

Acknowledgements

None.

Appendix A. Supplementary material

Supplementary data to this article can be found online at https://doi.org/10.1016/j.envint.2022.107649.

References

Abatzoglou, J.T., et al., 2018. TerraClimate, a high-resolution global dataset of monthly climate and climatic water balance from 1958–2015. Sci. Data 5 (1), 170191.
Abdussalam, A.F., et al., 2014. Climate Influences on Meningitis Incidence in Northwest Nigeria. Weather Clim. Soc. 6 (1), 62–76.
Abdussalam, A.F., et al., 2014. The Impact of Climate Change on Meningitis in Northwest Nigeria An Assessment Using CMIP5 Climate Model Simulations. Weather Clim. Soc. 6 (3), 371–379.
Adebayo, A.A., 2001. *Temperature variability and outbreak of meningitis and measles in Yola, Nigeria.* Global. J. Pure Appl. Sci. 7 (1), 133–136.
Analysis of the Effect of Temperature on Age and Sex Incidence of Cerebro-Spinal Meningitis in Funtua Local Government Area, Katsina State, Nigeria. 2021.
Ayanlade, A., et al., 2020. Early warning climate indices for malaria and meningitis in tropical ecological zones. Sci. Rep. 10 (1), 14303.
Bathiany, S., et al., 2018. Climate models predict increasing temperature variability in poor countries. Sci. Adv. 4 (5), eaar5809.
Black, C., et al., 2017. Wildfire smoke exposure and human health: Significant gaps in research for a growing public health issue. Environ. Toxicol. Pharmacol. 55, 186–195.
Buhari, B. Temperature Variability and Outbreak of Meningitis and Measles in Zaria, Northern Nigeria. 2011.
Codjoe, S.N., Nabie, V.A., 2014. Climate change and cerebrospinal meningitis in the Ghanaian meningitis belt. Int. J. Environ. Res. Public Health 11 (7), 6923–6939.
Collaborators, G.B.D.M., 2018. Global, regional, and national burden of meningitis, 1990–2016: a systematic analysis for the Global Burden of Disease Study 2016. Lancet Neurol. 17 (12), 1061–1082.
Collaborators, G.B.D.D., 2020. Global age-sex-specific fertility, mortality, healthy life expectancy (HALE), and population estimates in 204 countries and territories, 1950–2019: a comprehensive demographic analysis for the Global Burden of Disease Study 2019. Lancet 396 (10258), 1160–1203.
Cuevas, L.E., et al., 2007. Risk mapping and early warning systems for the control of meningitis in Africa. Vaccine 25, A12–A17.
Diseases, G.B.D., Injuries, C., 2020. Global burden of 369 diseases and injuries in 204 countries and territories, 1990–2019: a systematic analysis for the Global Burden of Disease Study 2019. Lancet 396 (10258), 1204–1222.
Erdem, H., et al., 2017. The burden and epidemiology of community-acquired central nervous system infections: a multinational study. Eur. J. Clin. Microbiol. Infect. Dis. 36 (9), 1595–1611.
Eyring, V., et al., 2016. Overview of the Coupled Model Intercomparison Project Phase 6 (CMIP6) experimental design and organization. Geosci. Model Dev. 9 (5), 1937–1958.
Fick, S.E., Hijmans, R.J., 2017. WorldClim 2: new 1-km spatial resolution climate surfaces for global land areas. Int. J. Climatol. 37 (12), 4302–4315.
Global Burden of Disease Collaborative Network. Global Burden of Disease Study 2019 (GBD 2019) Results. Seattle, United States: Institute for Health Metrics and Evaluation (IHME), 2020. Available from https://vizhub.healthdata.org/gbd-results/.
Greenwood, B.M., et al., 1984. Meningococcal disease and season in sub-Saharan Africa. Lancet 1 (8390), 1339–1342.
Harrison, L.H., Trotter, C.L., Ramsay, M.E., 2009. Global epidemiology of meningococcal disease. Vaccine 27 (Suppl 2), B51–B63.
Henne, P.D., et al., 2018. An empirical perspective for understanding climate change impacts in Switzerland. Reg. Environ. Chang. 18 (1), 205–221.
Kohil, A., et al., 2021. Viral meningitis: an overview. Arch. Virol 166 (2), 335–345.
Lavigne, E., Burnett, R.T., Weichenthal, S., 2018. Association of short-term exposure to fine particulate air pollution and mortality: effect modification by oxidant gases. Sci. Rep. 8 (1), 16097.
Lenton, T.M., et al., 2008. Tipping elements in the Earth's climate system. PNAS 105 (6), 1786–1793.
Lobell, D.B., Di Tommaso, S., Burney, J.A., 2022. Globally ubiquitous negative effects of nitrogen dioxide on crop growth. Sci. Adv. 8 (22), eabm9909.
Loh, E., et al., 2013. Temperature triggers immune evasion by Neisseria meningitidis. Nature 502 (7470), 237–240.
Ma, Y., et al., 2021. Linking climate and infectious disease trends in the Northern/Arctic Region. Sci. Rep. 11 (1), 20678.
Molesworth, A.M., et al., 2003. Environmental risk and meningitis epidemics in Africa. Emerg. Infect. Dis. 9 (10), 1287–1293.
Moore, P.S., 1992. Meningococcal meningitis in sub-Saharan Africa: a model for the epidemic process. Clin. Infect. Dis. 14 (2), 515–525.
Palmgren, H., 2009. Meningococcal disease and climate. Glob. Health Action 2.
Petrie, R., et al., 2021. Coordinating an operational data distribution network for CMIP6 data. Geosci. Model Dev. 14 (1), 629–644.
Pickering, L., et al., 2018. Long-term health and socioeconomic consequences of childhood and adolescent onset of meningococcal meningitis. Eur. J. Pediatr. 177 (9), 1309–1315.
H.-O. Pörtner, D.C.R., M. Tignor, E.S. Poloczanska, K. Mintenbeck, A. Alegría, M. Craig, S. Langsdorf, S. Löschke, V. Möller, A. Okem, B. Rama (eds.), *IPCC, 2022: Climate Change 2022: Impacts, Adaptation, and Vulnerability. Contribution of Working Group II to the Sixth Assessment Report of the Intergovernmental Panel on Climate Change*. Cambridge University Press. In Press.
Reid, C.E., et al., 2016. Critical Review of Health Impacts of Wildfire Smoke Exposure. Environ. Health Perspect. 124 (9), 1334–1343.
Shaposhnikov, D., et al., 2014. Mortality related to air pollution with the moscow heat wave and wildfire of 2010. Epidimiology 25 (3), 359–364.
Sultan, B., et al., 2005. Climate drives the meningitis epidemics onset in west Africa. PLoS Med. 2 (1), e6.
Tian, J., et al., 2021. Projections of precipitation over China based on CMIP6 models. Stoch. Env. Res. Risk A. 35 (4), 831–848.
van Deuren, M., P. Brandtzaeg, and J.W. van der Meer, *Update on meningococcal disease with emphasis on pathogenesis and clinical management.* Clin Microbiol Rev, 2000. **13** (1): p. 144-66, table of contents.
Wright, C., et al., 2021. The Global Burden of Meningitis in Children: Challenges with Interpreting Global Health Estimates. Microorganisms 9 (2).
Xu, R., et al., 2020. Wildfires, Global Climate Change, and Human Health. N. Engl. J. Med. 383 (22), 2173–2181.
Yaka, P., et al., 2008. Relationships between climate and year-to-year variability in meningitis outbreaks: a case study in Burkina Faso and Niger. Int. J. Health Geogr. 7, 34.
Zhao, G., et al., 2022. Evaporative water loss of 1.42 million global lakes. Nat. Commun. 13 (1), 3686.